Desalination and Water Treatment
www.deswater.com

27 (2011) 285–293
March

1944-3994/1944-3986 © 2011 Desalination Publications. All rights reserved
doi: 10/5004/dwt.2011.2031

Simulation of indigo carmine dye adsorption on polymer doped sawdust in fixed-bed systems

Deli Liu, Dezhi Sun*

School of Municipal and Environmental Engineering, Harbin Institute of Technology, Harbin 150090, PR China
Tel. +86 631 5687037; email: rensiyuan2004@126.com

Received 19 May 2010; Accepted 21 July 2010

ABSTRACT

This research analyzes the potential use of polyaniline doped sawdust (PANI/SD) as a low-cost adsorbent to remove indigo carmine (IC) from aqueous solutions in a continuous fixed-bed system. The effects of inlet dye flow rate, concentration and bed height on the breakthrough characteristics of the adsorption system were determined. The breakthrough time and saturation time increased with decreases in the flow rate and the inlet concentration. The same effect was shown when the bed depth was increased. The average bed adsorption capacity q_0 was 80.24 mg/g. The adsorption data were fitted to four well-established fixed-bed adsorption models: the Thomas, the Yoon–Nelson, the Adams–Bohart model and the bed-depth service time models (BDST). The results conformed to the Thomas and Yoon–Nelson models, with coefficients of correlation (R^2) ≥ 0.97 under different conditions. The breakthrough time and exhaustion time values predicted with the BDST model under different conditions agreed with the experimental values. PANI/SD was shown to be a suitable adsorbent for the adsorption of indigo carmine using a fixed-bed adsorption column.

Keywords: Adsorption; Dye; Sawdust; Fixed bed

1. Introduction

Dyes are commonly used in many industries and laboratories. Colored dye effluents pose a major threat to the surrounding ecosystem because the dyes interfere with the transmission of the light necessary for photosynthesis, causing a disturbance in the ecological systems of the receiving waters [1]. Among various dyes, indigo carmine (IC), an anionic dye is widely used as a colorant for food, pharmaceuticals and cosmetics, as an indicator in analytical chemistry, and as a microscopice stain in biology [2]. However, IC is considered a highly toxic indigoid class dye and that can cause skin and eye irritations in humans on contact. It also may cause gastrointestinal irritation with nausea, vomiting and diarrhea, and may cause respiratory tract irritation [3].

Various techniques have been employed for the removal of dyes from wastewater, such as coagulation and flocculation [4,5], biodegradation [6], chemical methods (chlorination and ozonation [7]), photocatalytic degradation processes [8,9], membrane separation [10] and adsorption [11,12]. Among the techniques used for dye removal, adsorption is one of the most effective measures for the decoloration and treatment of day wastewater. Several conventional adsorbents have been thoroughly investigated, including activated carbon [13], clay [14], ion exchange resins [15] and zeolite [16]. Low-cost adsorbents offer many promising benefits for commercial applications. Many agricultural residues, such as wheat straw, wood chips and corncobs [17,18]

*Corresponding author.

have been used successfully to adsorb individual dyes and dye mixtures in wastewater. In particular, sawdust, a cheap and abundant material, has been investigated as an adsorbent for removing dyes from wastewater. However, the adsorption capacity is relatively low even for salt, acid or alkali treated sawdust [19,20].

Polyaniline, a dark-blue powder, has received considerable attention in recent years because of its high environmental stability, high electrical conductivity and easy synthesis [21]. In addition, polyaniline is expected to have a strong affinity for anionic dyes due to its many amine and imine functional groups. Few studies examining the removal of dyes by polyaniline have been reported [22,23]. Unfortunately, polyaniline itself cannot be directly employed for the removal of dyes in fixed-bed or other flow-through systems due to the excessive pressure drop resulting from its fine particle size. Polyaniline was directly synthesized on the surface of sawdust as a composite adsorbent for the removal of IC. This composite can not only increase the adsorbent capacity of sawdust, but also improve the mechanical performance of polyaniline.

The aim of this study was to explore the use of polyaniline doped sawdust (PANI/SD) for the adsorptive removal of IC from wastewater. The effect of flow rate, influent concentration and bed depth on IC adsorption by a fixed-bed column was investigated. Thomas, Yoon–Nelson, Adams–Bohart and BDST models were used to predict the performance.

2. Materials and methods

2.1. Chemicals and reagents

Indigo carmine (IC), the chemical structure of which is shown in Fig. 1, was used without purification. The maximum wavelength adsorption of this dye is 586.5 nm. The dye solution was prepared by dissolving accurately weighted dye in deionized water. All other chemicals used in this study were analytical grade.

2.2. Preparation and character of adsorbent

The sawdust used was obtained from a local furniture manufacturing company. The specific surface area of the sawdust was measured using by a BET surface area analyzer. The values for specific surface area and pore diameter were 1.06 $m^2 g^{-1}$ and 0.68 μm, respectively. The average particle diameter of sawdust was 1.85 mm. The sawdust was washed to remove dust and other contaminants and then dried. The sawdust was added to an aniline solution in 1 M hydrochloric acid. Polymerization was initiated by the addition of an ammonium peroxydisulfate solution in 1 M hydrochloric acid with continuous stirring at room temperature. The mixture was kept for overnight to complete the reaction. The insoluble precipitate was filtered and washed with water until the filtrate was colorless. The dark-green colored PANI/SD was dried at 50 °C in an oven. The composition of the PANI/SD was 0.48 g polyaniline per gram of adsorbent.

The adsorbent was characterized by X-ray diffraction (XRD). The XRD spectra of PANI/SD are shown in Fig. 2. The XRD patterns were recorded on a XD–2 diffractometer with Cu K_α operated at 30 kV and 20 mA. The scanning scope and scanning speed were 10–90° and 2°/min, respectively.

Fourier transform infrared spectroscopy (FTIR) of the sawdust and PANI/SD were recorded using a Nicolet 380 Series FTIR Spectrometer. A weight of sample (2 mg) was mixed with 100 mg of FTIR-grade KBr. The samples were scanned at 4 cm^{-1} resolution in the 4000–400 cm^{-1} range. The FTIR spectra of sawdust and PANI/SD are shown in Fig. 3.

The FTIR spectra of sawdust showed peaks at 3400, 2930, 2360, 1626, 1450, 1420 and 1160 cm^{-1} which may be assigned to OH group, CH_2 especially alkenes, amide, C=O, CH deformation, OH deformation and OH stretch, respectively. The intensity of the peaks were either minimized or shifted in case of treated sawdust and the peaks of polyaniline can be seen.

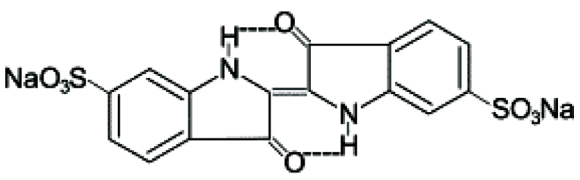

Fig. 1. Chemical structure of indigo carmine.

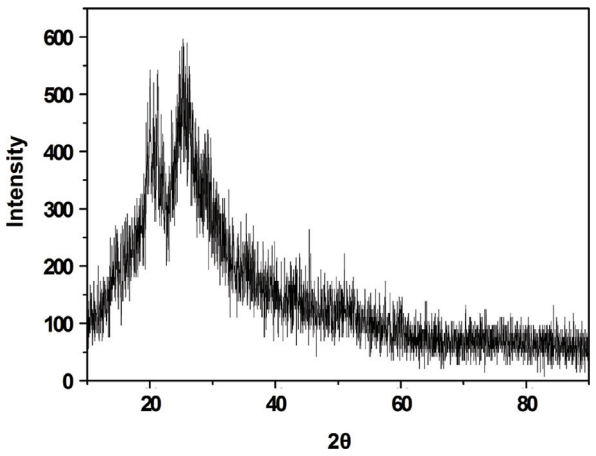

Fig. 2. XRD of polyaniline/sawdust.

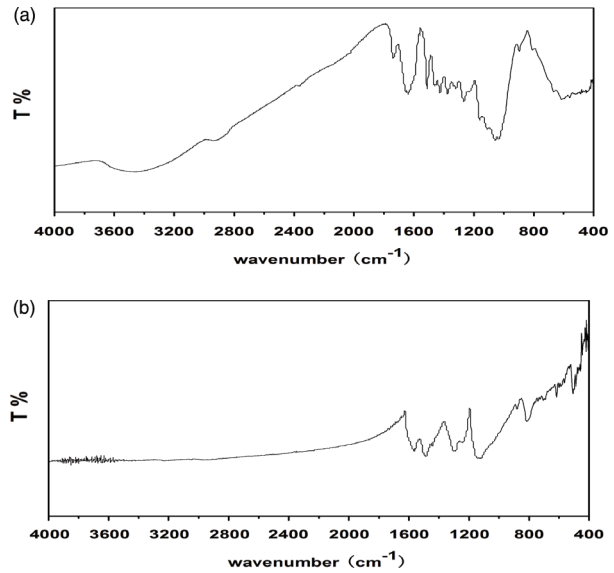

Fig. 3. FTIR spectra of (a) sawdust and (b) polyaniline doped sawdust.

2.3. Fixed-bed experiments and data analysis

The fixed-bed experiments were carried out in a water-jacketed glass column of 10 mm ID and 400 mm length at a constant temperature of 20 °C. The column was packed with different bed heights of PANI/SD on a glass–wool support. The experiments were performed at pH 5, which resulted from dissolving the dye in water without further pH adjustment. The batch experimental results showed that the adsorption rate was high at pH 5. A solution with a known concentration of IC was fed to the top of the column at the desired flow rate as regulated by a peristaltic pump. The samples in the outlet were collected and their concentrations were analyzed at approximately 10 min intervals. The effluent concentration was measured with a NEWLABO 2200 UV–visible spectrophotometer at 586.5 nm using a cell with a 1-cm optical path length. All samples were analyzed in triplicate. Because the diameter of the column is on average 12-fold greater than that of the sawdust particles, the effects of near-wall disturbances and preferential channels in the column can be neglected. The column studies were terminated when the column reached exhaustion.

The breakthrough curve shows the loading behavior of IC to be removed from solution in a fixed-bed column. It is expressed in terms of normalized concentration defined as the ratio of outlet to inlet IC concentration (C_t/C_0) as a function of time. Breakthrough time (t_B) is defined as the time which the IC concentration in the effluent is 1% of the concentration applied to the column. Exhaustion time (t_E) is defined as the time when the IC concentration in the effluent is 90% that of the applied concentration. Breakthrough volumes (V_B) and exhaustion volumes (V_E) are the effluent volume at breakthrough time and exhaustion time, respectively. In the present study, three main factors were considered: flow rate, bed depth and inlet dye concentration. For a given feed concentration and flow rate, the adsorption capacity of the bed, q_0 (mg/g), can be determined by integration

$$q_0 = \int_0^{V_t} \frac{(C_0 - C_t)}{W} dV = Q \int_0^{t} \frac{(C_0 - C_t)}{W} dt \quad (1)$$

where C_0 and C_t are the initial and effluent adsorbate concentration (mg/l), V is the volume of effluent (ml), V_t is the effluent volume at time t (ml), W is the mass of the adsorbent (g) and Q is the flow rate which circulates through the column in ml/min.

3. Results and discussion

3.1. Effect of feed flow rate

The effect of flow rate on the IC adsorption characteristics of PANI/SD in the continuous flow packed column was examined by varying the flow rate (6, 8, 10 ml/min) while the temperature and the dye concentration were held constant at 293 K and 100 mg/l, respectively. The quality of the adsorbent and the depth of the column were also unchanged. The breakthrough curve at various flow rates is shown in Fig. 4.

It can be seen from Fig. 4 that breakthrough generally occurred more quickly with a higher flow rate. Details of breakthrough time (t_B), exhaustion time (t_E) and adsorption capacity are presented in Table 1. Breakthrough

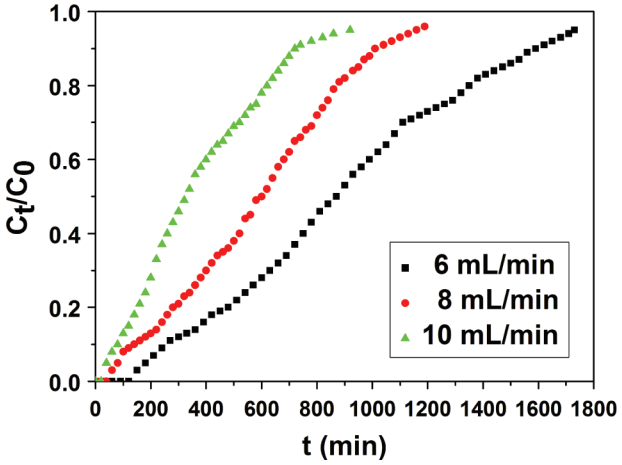

Fig. 4. IC adsorption breakthrough curve at three different flow rates.

Table 1
Column data parameters obtained at different flow rates, IC concentrations, bed heights and (T = 20 ± 1 °C)

Initial concentration (mg/l)	Flow rates (ml/min)	Bed height (cm)	q_0 (mg/g)	t_B (min)	V_B (l)	t_E (min)	V_E (l)
50	8	20	70.27	130	1.04	1500	12.0
100	8	20	77.64	50	0.40	1010	8.08
200	8	20	109.96	30	0.24	660	5.28
100	6	20	88.84	120	0.72	1590	9.45
100	10	20	61.73	20	0.20	720	7.2
100	8	15	64.77	30	0.24	630	5.04
100	8	25	88.49	70	0.56	1350	10.8

time and exhaustion time were increased significantly with a decrease in the flow rate. The breakthrough volumes (V_B) obtained for the 6, 8 and 10 ml/min flow rates were 0.72, 0.40 and 0.20 l, respectively, and their corresponding exhaustion volumes (V_E) were 9.45, 8.08 and 7.20 l, respectively. It was shown that breakthrough and exhaustion generally occurred more quickly with higher flow rate. The variation in the slopes of the breakthrough curve may be explained on the basis of mass transfer fundamentals. At a lower rate of influent, IC had more time to be in contact with adsorbent, which resulted in a greater adsorption capacity for IC molecules in the column. With the increase of flow rate, liquid–solid contact time was insufficient, and the solute left the column before equilibrium occurred. These results were in agreement with those reported in the literature [24,25].

3.2. Effect of bed height

To study the effect of bed height, experiments were conducted with three columns filled with 3.05, 4.6 and 6.1 g of adsorbent, which yielded respective bed heights 15, 20 and 25 cm, respectively, with a constant flow rate of 8 ml/min and an IC inlet concentration of 100 mg/l. Fig. 5 shows the breakthrough profile of IC adsorption at different bed heights. The column data and parameters obtained at different bed height are also listed in Table 1. The results in Fig. 5 show that an increase in column height resulted in an increase in breakthrough time and that the slope of breakthrough curve decreased with increasing in bed height. The steepness of the breakthrough curves was strongly related to the bed height. Increasing in bed height resulted in an increased contact time between the IC and PANI/SD and a corresponding increase in the amount of adsorbate uptake. Therefore, a higher bed column resulted in a decrease in the solute concentration in the effluent. Table 1 shows that IC uptake by PANI/SD calculated using Eq. (1), for bed heights of 15, 20 and 25 cm were 64.77, 77.64 and 88.49 mg/g.

3.3 Effect of inlet concentration

Fig. 6 shows the effect of feed concentration on the breakthrough curve for an adsorbent bed height of 20 cm and a solution flow rate of 8 ml/min. It can be

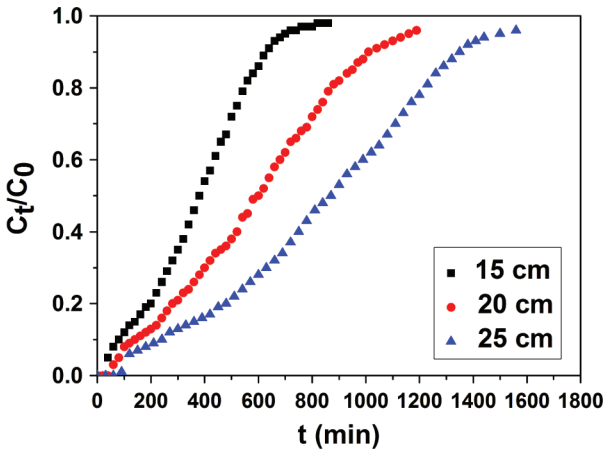

Fig. 5. IC adsorption breakthrough curve at three bed depths.

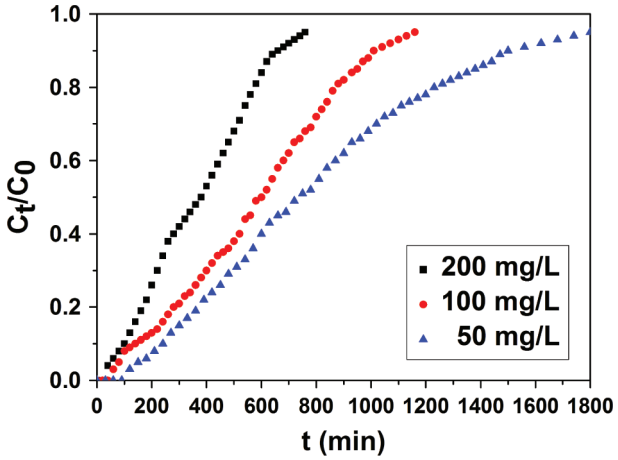

Fig. 6. IC adsorption breakthrough curve at three different inlet concentrations.

seen that, over a period of 200 min, the value of C_t/C_0 reached 0.07, 0.13 and 0.26 when the inlet concentration was 50, 100 and 200 mg/l, respectively. As influent concentration increased, breakthrough curves were sharper, and the column with the highest inlet concentration was more quickly saturated. This can be explained by a lower concentration gradient causing a slower transport due to a decrease in the diffusion coefficient or the mass transfer coefficient. These results are similar to those found by other researchers in columns using different sorbent materials [26].

In the following sections, the above experimental results have been fitted to four models with the aim to describe the behavior of the column and to determine the corresponding kinetic parameters.

3.4. Thomas model

The Thomas model assumes Langmuir kinetics of adsorption and desorption, and no axial dispersion. It is one of the most general and widely used models to describe the behavior of adsorption processes in fixed-bed columns. The model can be used to fit the experimental data to determine both the rate constant (k_{Th}) and the maximum solid phase concentration (q_0). The model is derived with the assumption that the rate driving force obeys second-order reversible reaction kinetics. The linearized form of the Thomas model is as follows:

$$\ln\left(\frac{C_0}{C_t}-1\right)=\frac{k_{Th}q_0W}{Q}-k_{Th}C_0t \quad (2)$$

where k_{Th} is the Thomas rate constant (ml/min mg), q_0 is the maximum solid phase concentration of the solute (mg/g), Q is the volumetric flow rate (l/min) and W is the mass of the adsorbent (g). The kinetic coefficient (k_{Th}) and the maximum solid phase concentration (q_0) can be determined from a plot of $\ln[(C_0/C) - 1]$ against t at a given flow rate.

This model was applied to the data between the breakthrough time and the exhaustion time of the column. The determined coefficients and relative constants were obtained using linear regression analysis according to Eq. (2) and the results are presented in Table 2. The values of the regression coefficient (R^2) indicate that the model describes the column performance data very well for the adsorption of IC ($R^2 > 0.97$).

With the increase in the inlet concentration and bed depth, the model rate constant (k_{Th}) decreased while the equilibrium adsorption capacity (q_0) increased. The decrease of k_{Th} is due to the increase of mass-transport resistance with increasing column bed depth and inlet concentration. The increase of q_0 is due to the increase of adsorption sites with the increasing bed depth [27]. With increasing inlet concentration, the concentration difference between the dye in solution and the dye on the adsorbent is enlarged and the driving force for adsorption is increased.

The bed capacity q_0 decreased and the coefficient k_{Th} increased with increasing flow rates. The results obtained were found to be similar to those reported previously by Uddin et al. [28]. The averaged uptake q_0 predicted by the Thomas model is 75.97 mg/g with a standard deviation of 4.27 mg/g, which is quite close to the averaged experimental value. The difference between the averaged experimental uptake and the average value predicted from the Thomas model was statistically insignificant. Therefore, the Thomas model can be considered as a suitable kinetic model to describe IC adsorption in a fixed bed of PANI/SD.

3.5. Yoon and Nelson model

The Yoon and Nelson model is a relatively simple model. This model assumes that the rate of decrease in the probability of adsorption for each adsorbate molecule is proportional to the probability of sorbate sorption and the probability of sorbate breakthrough on sorbent [29].

Table 2
Thomas and Yoon and Nelson model parameters at different conditions using linear regression analysis

Inlet concentration (mg/l)	Flow rate (ml/min)	Bed height (cm)	Thomas model			Yoon and Nelson model		
			k_{Th} (ml/min mg)	q_0 (mg/g)	R_2	k_{YN} (1/min)	τ (mg/g)	R^2
50	8	20	0.065	52.86	0.98	3.27×10^{-3}	806.1	0.98
100	8	20	0.050	77.71	0.99	5.03×10^{-3}	592.6	0.99
200	8	20	0.030	98.22	0.98	7.52×10^{-3}	374.5	0.98
100	6	20	0.034	89.28	0.99	3.37×10^{-3}	907.7	0.99
100	10	20	0.061	61.56	0.97	6.12×10^{-3}	375.5	0.97
100	8	15	0.081	64.17	0.99	8.13×10^{-3}	369.0	0.99
100	8	25	0.039	87.98	0.98	3.98×10^{-3}	835.8	0.98

The Yoon–Nelson equation for a single component system is expressed as Eq. (3):

$$\frac{C_t}{C_0} = 1 + \exp(k_{YN}(\tau - t) \quad (3)$$

where k_{YN} is the Yoon and Nelson's rate constant (min^{-1}) and τ is the time required for retaining 50% of the adsorbate breakthrough (min). The linearized form of the Yoon–Nelson model is given by Eq. (4):

$$\ln\left(\frac{C_t}{C_0 - C_t}\right) = k_{YN}t - \tau k_{YN} \quad (4)$$

This model was also been applied to the same range of effluent concentrations as for the Thomas model (between the breakthrough time and the saturation time). The values of k_{YN} and τ were determined from $\ln[C_t/(C_0 - C_t)]$ versus t at different operating conditions. The values of k_{YN} and τ are listed in Table 3. The rate constant k_{YN} increased and the 50% breakthrough time (τ) decreased with increasing flow rate. Similarly, the Yoon and Nelson constant (k_{YN}) varied between 3.24×10^{-3} and 7.52×10^{-3} min^{-1} when the concentration increased from 50 to 200 mg/l. The greater value for the rate constant when the inlet IC concentration is higher may be related to the increase in the forces that control the mass transfer in the liquid phase. With increasing bed heights, the values of τ increased while the values of k_{YN} decreased. The calculated τ values are quite similar to those obtained experimentally. With the Yoon–Nelson model, the values of the correlation coefficients (R^2) listed in Table 2 also provide a fit ($R^2 > 0.97$).

3.6. Adams–Bohart model

The Adams–Bohart model is used for the initial part of the breakthrough curve when the concentration $C_t < 0.5C_0$. The model is expressed by the following:

$$\ln\left(\frac{C_t}{C_0}\right) = k_{AB}C_0t - k_{AB}N_0\frac{Z}{u} \quad (5)$$

where C_0 and C_t are the initial and effluent adsorbate concentration (mg/l), k_{AB} is the kinetic constant (l/mg min), Z is the column bed depth of column (cm), N_0 is the saturation concentration (mg/l) and u is the linear flow rate (cm/min). A linear plot of $\ln(C_t/C_0)$ against time (t) was used to determine values of k_{AB} and N_0 from the intercept and slope of the plot. The results are presented in Table 3.

The values of k_{AB} decreased with both initial IC concentration and increased bed height, but it increased with flow rate increase. The results obtained were found to be similar to those reported previously by Han et al. [30]. The Adams–Bohart does not adequately reproduce in some cases the experimental data obtaining R^2 values less than 0.95.

3.7. Bed-depth service time (BDST) analysis model

3.7.1. Effect of bed depth

The BDST model is generated from the Adams–Bohart equation, and predicts a linear relationship between the bed depth and service time. It is based on the assumption that the rate of adsorption is controlled by the surface reaction between adsorbate and the unused capacity of the adsorbent [31].

$$t = \frac{N_0Z}{C_0u} - \frac{1}{k_{ads}C_0}\ln\left(\frac{C_0}{C_t} - 1\right) \quad (6)$$

where t is the service time (min), N_0 is the adsorption capacity per unit volume of bed (mg/l), Z is the depth of the adsorbent bed (cm), u is the linear flow rate (cm/s), C_0 and C_t are the influent and the effluent adsorbate concentration (mg/l), respectively, and k_{ads} is the adsorption rate constant (l/mg min). A plot of t versus Z can generate a straight line equation:

Table 3
Adams–Bohart parameters at different conditions using linear regression analysis

Inlet concentration (mg/l)	Flow rate (ml/min)	Bed height (cm)	k_{AB} (ml/min mg)	N_0 (mg/l)	R^2
50	8	20	0.758	2145.5	0.94
100	8	20	0.417	3631.2	0.92
200	8	20	0.349	4358.4	0.91
100	6	20	0.319	5192.1	0.93
100	10	20	0.758	1951.5	0.95
100	8	15	0.588	3250.3	0.96
100	8	25	0.280	4358.3	0.99

$$t_s = aZ - b \quad (7)$$

where a is the slope of the BDST line ($a = N_0/C_0 u$) and b is the intercept of this equation

$$b = -\frac{1}{k_{ads}C_0}\ln\left(\frac{C_0}{C_t} - 1\right) \quad (8)$$

Linear BDST plots for three bed column at 10%, 50% and 90% breakthrough (calculated from Fig. 4) are shown in Fig. 7. The values of k_{ads} and N_0 were calculated from the intercept and slope, and the results are shown in Table 4. It can be seen that the correlation coefficient values are all > 0.96, suggesting that the data fit the BDST model. With increasing breakthrough time, there was a consistent rise in slope and a subsequent increase in the corresponding dynamic adsorption capacity (N_0). The values of k_{ads} and N_0 indicate that the PANI/SD was highly efficient for the removal of IC from a water environment.

3.7.2. Design of adsorption column for different flow rates

According to the BDST model (Eq. (6)), the data collected from one flow rate experiment can used to predict the behavior of a system with a different flow rate.

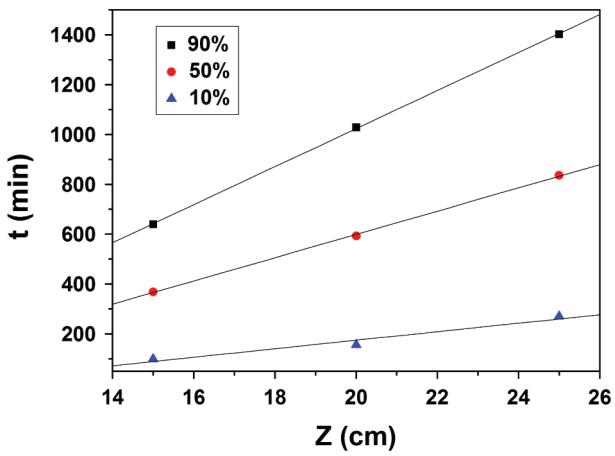

Fig. 7. BDST plot for IC adsorption at various breakthrough (Fig. 3 data was used).

Table 4
Coefficients of BDST equation

Breakthrough (%)	a	B	N_0 (mg/l)	k_{ads} (l/mg min)	R^2
10	17.08	–166.92	4351.59	0.0079	0.96
50	46.68	–334.54	11894.01	0	0.99
100	76.29	–502.14	19436.17	0.00261	0.99

If an experiment is conducted at flow rate Q_1, yielding an equation of the form:

$$t_s = a_1 Z - b_1 \quad (9)$$

then it is possible to predict the equation for flow rate Q_2 as follows:

$$a_2 = a_1 \frac{Q_1}{Q_2} \quad (10)$$

$$b_2 = b_1 \quad (11)$$

Columns were run with flow rates of 6 and 10 ml/min, whereas the original flow rate was 8 ml/min (Fig. 4). The breakthrough times (10%, 50% and 90%) were calculated by applying the data from a previous column study at a flow rate of 8 ml/min using Eq. (7).The results are shown in Table 5. The predicted values were comparable to the experimental values.

3.7.3. Design of adsorption column for different initial concentrations

The BDST model can also be used to design systems for other inlet concentration. When a laboratory test is conducted at solute concentration C_1, yielding an equation of the form

$$t_s = a_3 Z - b_3 \quad (12)$$

A new inlet concentration C_2 can be described by the equation

$$t_s = a_4 Z - b_4 \quad (13)$$

$$a_4 = a_3\left(\frac{C_1}{C_2}\right) \quad (14)$$

$$b_4 = b_3\frac{C_1}{C_2}\left(\frac{\ln[(C_2 / C_{t2}) - 1]}{\ln[(C_1 / C_{t1}) - 1]}\right) \quad (15)$$

The column was run with initial IC concentrations of 50 and 200 mg/l, whereas the original concentration was 100 mg/l (Fig. 6). The flow rate was kept at 8 ml/min and the column depth was kept 20 cm. Using Eqs. (14) and (15), theoretical slopes and intercepts were determined and breakthrough times (10%, 50% and 90%) for the two concentrations were calculated (Table 5). The predicted times were in good agreement with the experimental breakthrough times.

Table 5
Comparison of experimental and theoretical breakthrough time using BSDT model

	Breakthrough 10%		Breakthrough 50%		Breakthrough 90%	
	t_{exp} (min)	t_{theo} (min)	t_{exp} (min)	t_{theo} (min)	t_{exp} (min)	t_{theo} (min)
Flow rate 6 ml/min	255.0	288.5	870.0	907.7	1590.0	1532.2
Flow rate 10 ml/min	80.0	106.4	335.0	412.4	720.0	718.4
Initial IR 75 mg/l	240.0	232.9	745.0	798.8	1500.0	1364.8
Initial IR 150 mg/l	100.0	116.5	380.0	399.0	660.0	680.0

4. Conclusion

This study evaluated the performance of polymer doped fixed bed systems for the removal of IC from aqueous solution. Polyaniline was directly synthesized on the surface of sawdust by the addition of an ammonium peroxydisulfate in aniline solution under acidic conditions. This polyaniline/sawdust was used as an adsorbent in fixed-bed columns. The results of this study show that PANI/SD can efficiently remove IC dye from waste water. Removal of IC using the doped sawdust is dependent on the influent flow rate, dye concentration and the bed height. The following conclusions can be drawn from the results of experiments in fixed bed column:

(1) As the flow rate is increased, the breakthrough curve becomes steeper. The break point time and exhaustion point time are obtained earlier. The fixed-bed adsorption capacity q_0 is decreased. The same results are obtained with the decrease in bed depth from 15 cm to 25 cm.
(2) For larger inlet concentration, steeper breakthrough curves are obtained and break point time and exhaustion point time are achieved faster. However the adsorption capacity q_0 is increased.
(3) For IC adsorption, the column data fit well to the Thomas and Yoon–Nelson models.
(4) BDST plots can be used to predict the breakthrough time of any column based on previously collected data from other columns. The predicted time show good correspondence with the experiment values of breakthrough time.

Symbols

a — Slope of BDST equation
b — Intercept of BDST equation
C_t — Effluent adsorbate concentration (mg/l)
C_0 — Inlet (feed) or initial concentration of dye in the aqueous phase (mg/l)
k_{AB} — Adams–Bohart model rate constant (l/min mg)
k_{Th} — Thomas rate constant (ml/min mg)
k_{YN} — Yoon and Nelson's rate constant (min^{-1})
N_0 — Adsorption capacity per unit bed volume (mg/l)
q_0 — Bed adsorption capacity of the bed (mg/g)
Q — Flow rate (ml/min)
R — Coefficient of correlation
t — Time (min)
t_B — Time at breakthrough (min)
t_E — Time at exhaustion (min)
T — Solution temperature (K)
u — Linear flow rate (cm/min)
V — Volume of effluent (l)
V_t — Effluent volume at time t (l)
V_B — Throughput volume (l)
V_E — Exhaustion volume (l)
W — Weight of adsorbent (g)
Z — Height of the bed (cm)

Greeks

T — Time required for retaining 50% of the adsorbate breakthrough (min)

References

[1] S.M.D. Brito and H.M.C. Andrade, J. Hazard. Mater., 174 (2010) 84–92.
[2] A. Mittal, J. Mittal and L. Kurup, J. Hazard. Mater., 137 (2006) 591–602.
[3] E. Gutierrez-Segura, M. Solache-Rios and A. Colin-Cruz, J. Hazard. Mater., 170 (2009) 1227–1235.
[4] C. Phalakornkule, S. Polgumhang and W. Tongdaung, J. Environ. Manag., 91 (2010) 918–926.
[5] M. Riera-Torres, C. Gutierrez-Bouzan and M. Crespi, Desalination, 252 (2010) 53–59.
[6] Y.X. Liu, J. Huang and X.Y. Zhang, J. Biosci. Bioeng., 108 (2009) 496–500.
[7] M.H. Phe, M. Dossot and J.C. Block, Water Res., 38 (2004) 3729–3737.
[8] L. Gao, Y.K. Zhai and H.Z. Ma, Appl. City Sci., 46 (2009) 226–229.
[9] L.G. Devi and K.M. Reddy, Appl. Surf. Sci., 256 (2010) 3116–3121.
[10] S. Sachdeva and A. Kumar, J. Membr. Sci., 329 (2009) 2–10.
[11] W.H. Zou, P. Han and Y.L. Lia, Desal. Water Treat., 12 (2009) 210–218.
[12] E. Eren, O. Cubuk and H. Ciftci, Desalination, 252 (2010) 88–96.
[13] E.N. El Qada, S.J. Allen and G.A. Walker, Chem. Eng. J., 135 (2008) 174–184.
[14] P. Liu and L.X. Zhang, Sep. Purif. Technol., 58 (2007) 32–39.

[15] G. Bayramoglu, B. Altintas and M.Y. Arica, Chem. Eng. J., 152 (2009) 339–346.
[16] B. Armagan, M. Turan and M.S. Celik, Desalination, 170 (2004) 33–39.
[17] H. Aydin, G. Baysal and Y. Bulut, Desal. Water Treat., 2 (2009) 139–147.
[18] M.M.A. El-Latif and A.M. Ibrahim, Desal. Water Treat., 6 (2009) 252–268.
[19] S.D. Khattri and M.K. Singh, J. Hazard. Mater., 167 (2009) 1089–1094.
[20] F.A. Batzias and D.K. Sidiras, Biores. Technol., 98 (2007) 1208–1217.
[21] P.A. Kumar, S. Chakraborty and M. Ray, Chem. Eng. J., 141 (2008) 130–137.
[22] D. Mahanta, G. Madras and S. Radhakrishnan, J. Phys. Chem. B, 112 (2008) 10153–10157.
[23] D. Mahanta, G. Madras and S. Radhakrishnan, J. Phys. Chem. B, 113 (2009) 2293–2299.
[24] A.A. Ahmad and B.H. Hameed, J. Hazard. Mater., 175 (2010) 298–303.
[25] V.C. Taty-Costodes, H. Fauduet and C. Porte, J. Hazard. Mater., B 123 (2005) 135–144.
[26] M. Calero, F. Hernáinzl and G. Blázquez, J. Hazard. Mater., 171 (2009) 886–893.
[27] S. Debnath, K. Biswas and U.C. Ghosh, Indus.l Eng. Chem. Res., 49 (2010) 2031–2039.
[28] M.T. Uddin, M. Rukanuzzaman and M.M.R. Khan, J. Environ. Manage., 90 (2009) 3443–3450.
[29] S. Kundu and A.K. Gupta Chem. Eng. J., 129 (2007) 123–131.
[30] R.P. Han, L.N. Zou and X. Zhao, Chem. Eng. J., 149 (2009) 123–131.
[31] J. Goel, K. Kadirvelu and C. Rajagopal, J. Hazard. Mater., 125 (2005) 211–220.